Potential Structural Biomarkers in 3D Images Validated by the First Functional Biomarker for Early Age-Related Macular Degeneration – ALSTAR2 Baseline

Sohaib Fasih-Ahmad,[1] Ziyuan Wang,[1] Zubin Mishra,[1] Charles Vatanatham,[1] Mark E. Clark,[2] Thomas A. Swain,[2,3] Christine A. Curcio,[2] Cynthia Owsley,[2] SriniVas R. Sadda,[1] and Zhihong Jewel Hu[1]

[1]Doheny Eye Institute, Pasadena, California, United States
[2]Ophthalmology and Visual Sciences, Heersink School of Medicine, University of Alabama at Birmingham, Birmingham, Alabama, United States
[3]Epidemiology, School of Public Health, University of Alabama at Birmingham, Birmingham, Alabama, United States

Correspondence: Zhihong Jewel Hu, Doheny Eye Institute, 150 North Orange Grove Blvd, Pasadena, CA 91103, USA;
jhu@doheny.org.

Received: September 10, 2023
Accepted: December 31, 2023
Published: February 1, 2024

Citation: Fasih-Ahmad S, Wang Z, Mishra Z, et al. Potential structural biomarkers in 3D images validated by the first functional biomarker for early age-related macular degeneration – ALSTAR2 baseline. *Invest Ophthalmol Vis Sci.* 2024;65(2):1.
https://doi.org/10.1167/iovs.65.2.1

Purpose. Lack of valid end points impedes developing therapeutic strategies for early age-related macular degeneration (AMD). Delayed rod-mediated dark adaptation (RMDA) is the first functional biomarker for incident early AMD. The relationship between RMDA and the status of outer retinal bands on optical coherence tomography (OCT) have not been well defined. This study aims to characterize these relationships in early and intermediate AMD.

Methods. Baseline data from 476 participants was assessed including eyes with early AMD (n = 138), intermediate AMD (n = 101), and normal aging (n = 237). Participants underwent volume OCT imaging of the macula and rod intercept time (RIT) was measured. The ellipsoid zone (EZ) and interdigitation zone (IZ) on all OCT B-scans of the volumes were segmented. The area of detectable EZ and IZ, and mean thickness of IZ within the Early Treatment Diabetic Retinopathy Study (ETDRS) grid were computed and associations with RIT were assessed by Spearman's correlation coefficient and age adjusted.

Results. Delayed RMDA (longer RIT) was most strongly associated with less preserved IZ area ($r = -0.591$; $P < 0.001$), followed by decreased IZ thickness ($r = -0.434$; $P < 0.001$), and EZ area ($r = -0.334$; $P < 0.001$). This correlation between RIT and IZ integrity was not apparent when considering normal eyes alone within 1.5 mm of the fovea.

Conclusions. RMDA is correlated with the status of outer retinal bands in early and intermediate AMD eyes, particularly, the status of the IZ. This correlation is consistent with a previous analysis of only foveal B-scans and is biologically plausible given that retinoid availability, involving transfer at the interface attributed to the IZ, is rate-limiting for RMDA.

Keywords: rod-mediated dark adaption (RMDA), age-related macular degeneration (AMD), ellipsoid zone (EZ), interdigitation zone (IZ), optical coherence tomography (OCT), retinal layer integrity, photoreceptor outer segments, retinal pigment epithelium (RPE), retinoids

Age-related macular degeneration (AMD) is a leading cause of irreversible central vision impairment worldwide[1] and subsequently causes significant psychological and socioeconomic burden due to depression, anxiety, and difficulty reading and driving.[2–4] Currently, strategies to reduce this burden focus on preventing or stabilizing end-stage neovascular and atrophic processes.[5] However, the vast majority of individuals with AMD have early disease[6] and there are no proven means to arrest the progression of early AMD, nor prevention strategies for those at high risk. A key barrier to developing preventative and therapeutic strategies is the lack of valid and responsive end points.[7]

Optical coherence tomography (OCT) is currently used to visualize 3D changes in retinal structure. In AMD, OCT biomarkers are used for diagnosis, management, and for monitoring progression of the disease.[8,9] This study concentrates on two hyper-reflective bands seen on OCT termed the ellipsoid zone (EZ) and interdigitation zone (IZ) based on current consensus nomenclature.[10,11] OCT segmentation can be a time-consuming and tedious process.[12] Therefore, we applied a novel, deep-learning-derived, graph-based algorithm[13] that was manually corrected to adequately analyze a large sample of OCT B-scans in an efficient yet accurate manner.

For regulatory approval, novel imaging biomarkers should have biologic plausibility by providing a biologic, physiologic, or pathologic pathway for the association of the biomarker with the disease and should have a contextual linkage between a biomarker and its intended use.[14] The current understanding of the hyper-reflective EZ signal in spectral domain OCT is that it is dominated by mitochondria in photoreceptor inner segments,[15–17] and mitochondrial dysfunction contributes to the outer retinal degeneration seen in AMD.[18–20] Further, the hyper-reflective IZ signal is attributed to the interface of photoreceptor outer segments, apical processes of the retinal pigment epithelium (RPE) and the surrounding interphotoreceptor matrix.[21] The RPE supports the photoreceptors at this interface by transferring substances locally produced by the RPE or substances ultimately derived from circulation, such as retinoids, that are required for phototransduction and photoreceptor health.[22]

Delayed rod-mediated dark adaptation (RMDA) is a slower return to rod-mediated sensitivity, measured as rod-intercept time (RIT), following a bright light flash stimulus. RMDA was established as a functional biomarker for incipient early AMD by the Alabama Study on Age-related Macular Degeneration (ALSTAR).[23] The retina has the highest metabolic demand in the body and this metabolic demand is even greater in the dark when ionic currents are flowing into the outer segments.[24–26] Given this metabolic demand in transitioning to the dark, it is plausible that mitochondrial dysfunction may play a role in delayed RMDA. Additionally, RMDA entails multiple steps which include retinoid transfer from RPE to photoreceptors, and retinoid availability is a rate-limiting for the speed of RMDA.[27,28] Consequently, one might hypothesize that delayed RMDA may be closely associated with changes in the EZ and IZ on OCT. Whereas the EZ has been shown to correlate with visual acuity,[29] the relationships between EZ integrity and RMDA, as well as IZ integrity and RMDA, have not been well-defined.

In this study, we utilize automated OCT segmentation with manual correction to explore the potential of the EZ and IZ area on OCT as an imaging biomarker for early AMD by measuring their association with delayed RMDA.

Methods

Methods pertaining to ALSTAR2 enrollment, inclusion and exclusion criteria, and functional testing are available in the Supplementary Materials.

De-identified raw OCT B-scan volumes were imported into 3D-OCTOR, a previously described and validated spectral domain OCT reading center grading software.[30–32] A novel deep-learning-derived graph-based algorithm was applied to segment the inner and outer boundaries of the IZ and the outer boundary of the EZ.[13] Boundaries of retinal layers generated by our algorithm were able to detect the absence of the IZ and EZ, particularly absence of IZ and EZ due to the presence of drusen or subretinal drusenoid deposits (SDD). This is because the upper boundary of the IZ or EZ will be below the upper boundary of the drusen and SDD thus eliminating that area of either the IZ or EZ and yielding a thickness of zero. Errors in automated segmentation were manually corrected and the boundaries were deleted if either band (EZ or IZ) was not clearly discernible in a region of scan, by a trained, masked grader (author C.V.). The segmentations were than reviewed by a second masked grader (author S.F.A.) and discrepancies were resolved by a principal investigator (author S.S.).

For the EZ, the inner border of the hyper-reflective EZ band was segmented by the algorithm and then manually adjusted as needed by the grader. The inner border of the EZ was defined as the hyper-reflective pixel immediately subjacent to the overlying hyporeflective pixel of the myoid zone. If the grader was unable to distinguish the hyper-reflective EZ band from the hyporeflective band of the myoid zone

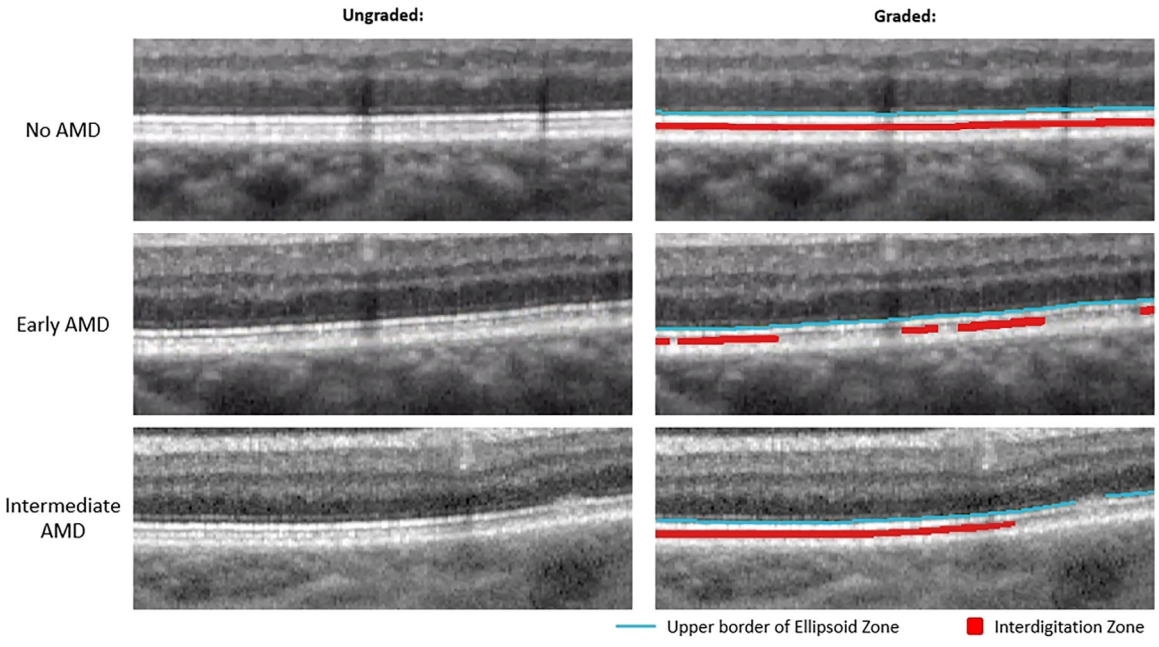

Figure 1. Magnified view of outer retinal bands in no AMD, early AMD, and intermediate AMD eyes. *Left*: Unaltered magnified OCT B-scans. *Right*: Same magnified OCT B-scan as the left side but graded for EZ and IZ. The *blue line* is the upper border of the EZ which was used as a proxy for discernable EZ, and the *red area* represents discernable IZ.

Investigative Ophthalmology & Visual Science

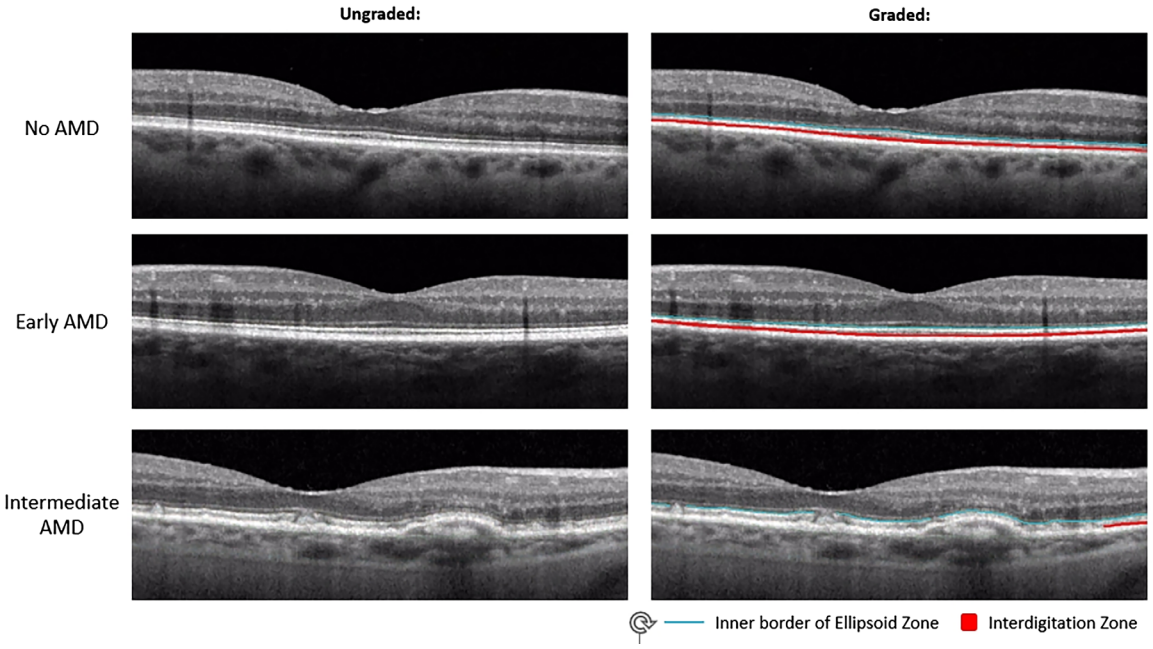

Figure 2. Magnified view of outer retinal bands on foveal B-scans in no AMD, early AMD, and intermediate AMD eyes. *Left*: Unaltered magnified OCT B-scans. *Right*: Same magnified OCT B-scan as the left side but graded for EZ and IZ. The *blue line* is the upper border of the EZ which was used as a proxy for discernable EZ, and the *red area* represents discernable IZ.

or the unnamed hyporeflective band between the EZ and IZ at any point on the B-scan, the segmentation was deleted. Subsequently, the area of EZ on that portion of the B-scan and half the distance to each adjacent B-scan was considered not discernible or not preserved.

Similarly, for the IZ, both the inner and outer boundaries were segmented by the algorithm and manually adjusted by the grader. The inner boundary of the IZ was defined as the hyper-reflective pixel subjacent to the overlying hyporeflective band between the EZ and IZ. The outer boundary was defined as the hyper-reflective pixel suprajacent to the underlying hyporeflective band between the IZ and RPE. If the grader was unable to distinguish between the IZ and either the underlying or overlying hyporeflective bands, the inner boundary was merged with the outer boundary. This results in the area of IZ on that portion of B-scan and half the distance to each adjacent B-scan to be considered not discernible (or not preserved), with a thickness of zero.

Figure 1 demonstrates examples of EZ and IZ grading in no AMD, early AMD, and intermediate AMD eyes. Figure 2 shows further examples of EZ and IZ grading in normal, early AMD, and intermediate AMD eyes on B-scans that include the fovea.

Mean area of IZ, mean thickness of IZ, and mean area of EZ were computed in the entire fovea-centered Early Treatment of Diabetic Retinopathy Study (ETDRS) grading grid,[33] as well as within the central subfield, inner ring, and outer ring of the ETDRS grid, as implemented in the Spectralis software (radii of 0.5, 1.0–1.5, and 1.5–3.0 mm, respectively). These regions were selected for analysis in all ALSTAR2 studies due to the radial symmetry of histologic rod loss in aging and AMD, that is, occurring in an annulus 0.5 to 3 mm from the foveal center, which was in turn defined by the point of highest cone density.[34,35] Separate means were calculated for each of the 3 groups based on AREDS 9-step classification system[36]: normal, early AMD, and intermediate AMD. Differences in the groups were assessed using analysis of covariance (ANCOVA). The relationships among RIT and the IZ area, the IZ thickness, and the EZ area were assessed using Spearman correlation coefficients (r) and were age-adjusted. Spearman correlation coefficients were calculated for the entire ETDRS grid as well as the central, superior inner, and superior outer subfields for each of the three groups (normal eyes, early AMD, and intermediate AMD). The level of significance was $P \leq 0.05$ (2-sided).

Results

A total of 476 eyes were assessed, of which 237 were classified as no AMD, 138 were classified as early AMD, and 101 were classified as intermediate AMD. Demographics of this population are shown in Table 1.

The area of EZ on OCT is reduced in eyes with intermediate AMD (27.699 mm^2) compared to eyes with early AMD (28.246 mm^2) and is reduced in eyes with

Table 1. Demographic Characteristics of Participants (n = 476)

Variable Names and Groups	Mean	SD or n %
Age (y)	71.75	5.88
Age group		
60–69 y	166	34.87
70–79 y	265	55.67
80–89 y	45	9.45
Gender		
M	192	40.34
F	284	59.66
Race		
White	431	90.55
Black	40	8.40
Other*	5	1.05

SD, standard deviation.
* Other includes 4 Asians or Pacific Islanders and 3 Native Americans.

Investigative Ophthalmology & Visual Science

Table 2A. Area of Preserved EZ/IZ in mm^2 and Correlation Between RMDA and EZ/IZ Areas in the Entire Grid, Central Subfield, and Inner and Outer Rings of the ETDRS Grid in all Eyes and Subdivided by AREDS Categories (Normal, Early AMD, and Intermediate AMD Eyes)

			Correlation of RMDA at 5 Degrees With Area of EZ and IZ				
			Area (mm^2)			Correlation	
Layer	ETDRS Subfield	AREDS Category	Mean	Std Dev	*P* Value	Correlation coefficient (*r*)	*P* Value
Ellipsoid zone (EZ)	Entire grid	All	28.149	0.068		**−0.334**	**<0.0001**
		Normal	28.270	0.023	<0.0001	**−0.199**	**0.002**
		Early	28.246	0.111		**−0.272**	**0.001**
		Intermediate	27.699	1.423		**−0.268**	**0.007**
	Central subfield	All	0.774	0.065		**−0.217**	**<0.0001**
		Normal	0.790	0.003	<0.0001	−0.055	0.401
		Early	0.787	0.014		−0.039	0.652
		Intermediate	0.752	0.088		−0.033	0.743
	Inner ring	All	6.232	0.281		**−0.348**	**<0.0001**
		Normal	6.280	0.011	<0.0001	−0.021	0.746
		Early	6.273	0.041		−0.117	0.175
		Intermediate	6.088	0.373		**−0.227**	**0.023**
	Outer ring	All	21.0893	1.058		**−0.292**	**<0.0001**
		Normal	21.2091	0.016	<0.0001	**−0.291**	**<0.0001**
		Early	21.1947	0.079		**−0.322**	**<0.0001**
		Intermediate	20.8628	1.128		**−0.258**	**0.010**
Interdigitation zone (IZ)	Entire grid	All	27.125	3.219		**−0.591**	**<0.0001**
		Normal	28.250	0.136	<0.0001	**−0.442**	**<0.0001**
		Early	27.909	0.777		**−0.496**	**<0.0001**
		Intermediate	23.223	5.538		**−0.472**	**<0.0001**
	Central subfield	All	0.707	0.192		**−0.531**	**<0.0001**
		Normal	0.789	0.011	<0.0001	−0.069	0.288
		Early	0.766	0.065		**−0.257**	**0.001**
		Intermediate	0.436	0.288		**−0.288**	**0.004**
	Inner ring	All	5.863	1.060		**−0.584**	**<0.0001**
		Normal	6.275	0.032	<0.0001	−0.107	0.101
		Early	6.173	0.235		**−0.303**	**<0.0001**
		Intermediate	4.397	1.646		**−0.414**	**<0.0001**
	Outer ring	All	20.555	2.190		**−0.538**	**<0.0001**
		Normal	21.195	0.122	<0.0001	**−0.460**	**<0.0001**
		Early	20.974	0.637		**−0.460**	**<0.0001**
		Intermediate	18.389	4.125		**−0.450**	**<0.0001**

P-values that indicate statistical significance (*P* values < 0.05) are in bold

early AMD compared to eyes without AMD (28.270 mm^2) in the entire ETDRS grid as well as each of the subfields that were analyzed (Table 2). The reduction in EZ area between early AMD and normal eyes is not statistically significant. Figure 3 demonstrates the en face maps generated by 3D-OCTOR representing the area of

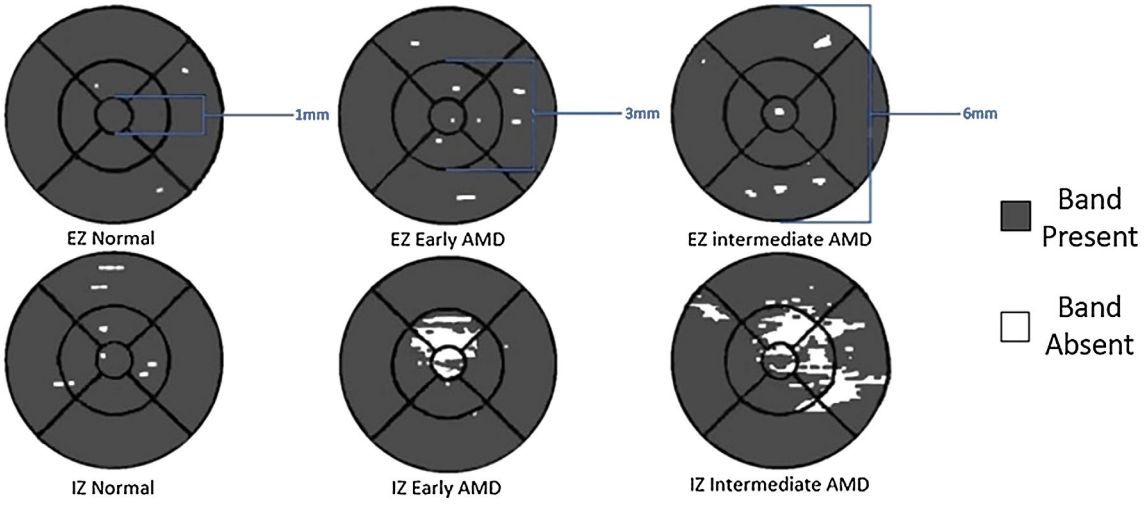

Figure 3. En face maps of the EZ and IZ in a normal aging, early AMD, and intermediate AMD eye within the ETDRS grid. The diameter of each subsection (central subfield, inner ring, and outer ring) are labeled in *blue*. The *white regions* indicate absence of the band (EZ or IZ); the *gray region* indicates the areas where the band is present.

Investigative Ophthalmology & Visual Science

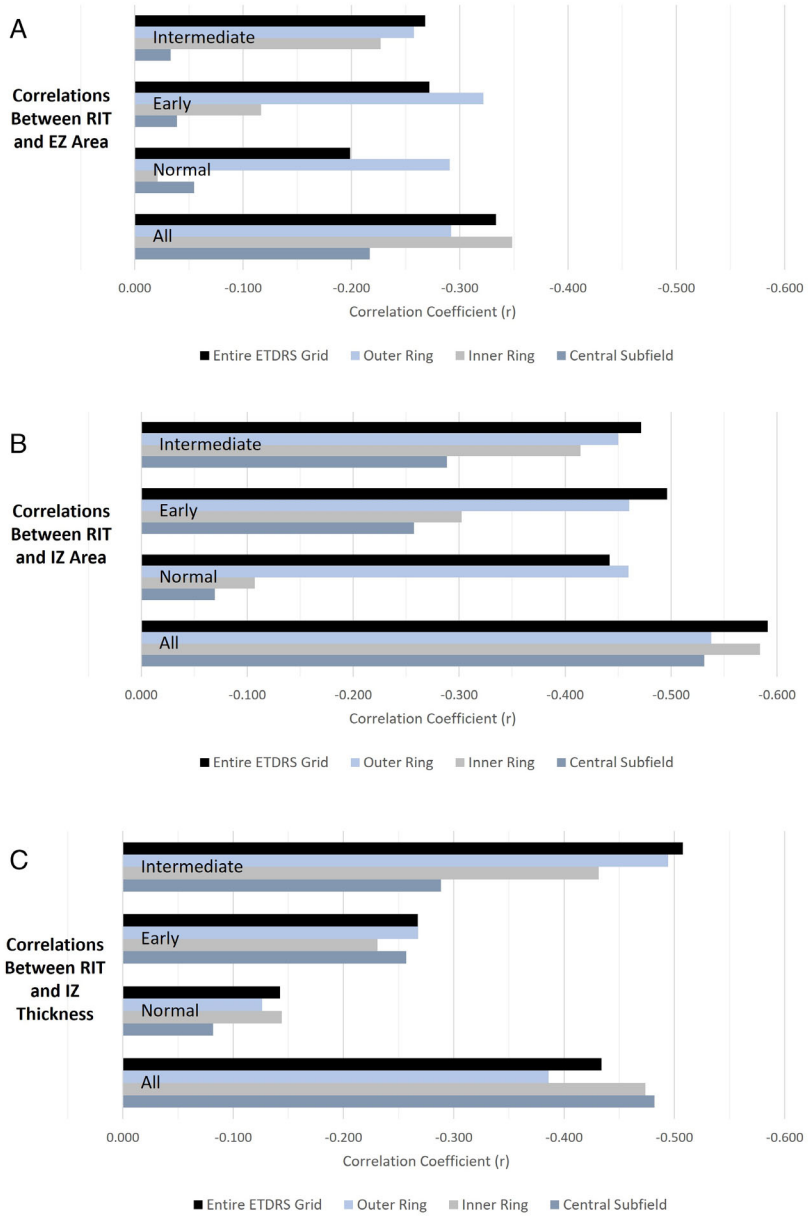

Figure 4. (**A**) Correlations between RIT and EZ area in the entire ETDRS grid, outer and inner rings, and central subfield of the ETDRS grid for all eyes, and only normal, early AMD and intermediate AMD eyes. (**B**) Correlations between RIT and IZ area in the entire ETDRS grid, outer and inner rings, and central subfield of the ETDRS grid for all eyes, and only normal, early AMD and intermediate AMD eyes. (**C**) Correlations between the RIT and mean IZ thickness in the entire ETDRS grid, outer and inner rings, and central subfield of the ETDRS grid for all eyes, and only normal, early AMD and intermediate AMD eyes.

EZ and IZ within the ETDRS grid and the associated subfields.

Slower RMDA (longer RIT) was associated with less preserved EZ area ($r = -0.334$) in the entire ETDRS grid. The strength of this association was diminished, but still present, when considering each of the Age-Related Eye Disease Study (AREDS) categories separately. Likewise, the same association was observed in each of the ETDRS subfields that were considered, and these associations were weaker than that of the entire ETDRS grid. In the central subfield, no correlation between the EZ area and RIT was found when considering eyes in each of the AREDS categories separately. In the inner ring, slower RMDA was associated with less preserved EZ area only in eyes with intermediate AMD. In the outer ring, a similar association was observed with all eyes considered and in each of the AREDS categories considered separately. Table 2A and Figure 4 show the associations for the various evaluated subfields.

Similar to the EZ, the area of IZ on OCT is decreased in eyes with intermediate AMD (23.233 mm^2) compared to eyes with early AMD (27.909 mm^2) and is decreased in eyes with early AMD compared to eyes without AMD (28.250 mm^2) in the entire ETDRS grid as well as each of the analyzed subfields (see Table 2). However, differences in the IZ area of normal and early AMD eyes were not statistically significant.

Investigative Ophthalmology & Visual Science

Table 2B. Mean Thickness of IZ in µm and Correlation Between RMDA and IZ in the Entire Grid, Central Subfield, and Inner and Outer Rings of the ETDRS Grid in all Eyes and Subdivided by AREDS Categories (Normal, Early AMD, and Intermediate AMD)

			Correlation of RMDA at 5 Degrees With Mean Thickness of IZ				
			Mean Thickness (µm)			Correlation	
Layer	ETDRS Subfield	AREDS Category	Mean	Std Dev	*P* Value	Correlation Coefficient (*r*)	*P* Value
Interdigitation zone (IZ)	Entire grid	All	16.221	4.093		**−0.434**	**<0.0001**
		Normal	16.983	3.572	<0.0001	**−0.142**	**0.029**
		Early	17.043	3.580		**−0.267**	**0.002**
		Intermediate	13.396	4.848		**−0.508**	**<0.0001**
	Central subfield	All	16.295	5.947		**−0.482**	**<0.0001**
		Normal	18.245	3.723	<0.0001	−0.082	0.210
		Early	18.225	4.428		**−0.257**	**0.002**
		Intermediate	9.505	7.174		**−0.288**	**0.004**
	Inner ring	All	15.734	4.684		**−0.474**	**<0.0001**
		Normal	16.987	3.731	<0.0001	**−0.144**	**0.027**
		Early	17.000	3.746		**−0.231**	**0.007**
		Intermediate	11.257	5.480		**−0.431**	**<0.0001**
	Outer ring	All	16.362	4.101		**−0.386**	**<0.0001**
		Normal	16.987	3.731	<0.0001	−0.126	0.053
		Early	17.043	3.598		**−0.268**	**0.002**
		Intermediate	14.238	5.091		**−0.494**	**<0.0001**

P-values that indicate statistical significance (*P* values < 0.05) are in bold

In addition, slower RMDA was associated with reduced IZ area for the entire ETDRS grid as well ($r = -0.591$) and this association was stronger than that between EZ and RIT. This association was again weaker when each of the AREDS categories was considered separately but still notable with correlations of $r = -0.442$ in normal eyes, $r = -0.496$ in early AMD eyes, and $r = -0.472$ in intermediate AMD eyes.

In the central subfield and inner ring, there was no association between the IZ area and RIT in normal eyes. There was an association between slower RMDA and IZ area in early AMD and intermediate AMD eyes, but these correlations were notably weaker than the association when considering the entire ETDRS grid.

Conversely, in the outer ring, the association between the slower RMDA and the IZ area was observed in normal eyes ($r = -0.460$) and this association was very similar in early AMD eyes ($r = -0.460$) and intermediate AMD eyes ($r = -0.450$). Additionally, this association was stronger in the outer ring than in the inner ring or central subfield when each AREDS category was considered separately, but weaker than the association observed while considering the entire grid except in normal eyes.

Associations between slower RMDA and mean thickness of the IZ were also observed for the entire ETDRS grid ($r = -0.434$) as well as for each of the subfields we analyzed (see Table 2B). Notably, these associations were weaker than those between the IZ area and RIT. As for the EZ and IZ areas, the associations between RIT and IZ thickness were stronger in eyes with intermediate AMD compared to eyes with early AMD and stronger in eyes with early AMD compared to eyes without AMD. Furthermore, the association between IZ thickness and RIT was strongest in the central subfield, followed by the inner ring and then the outer ring.

Discussion

In this study, we explored the structure-function relationship between preserved area of the EZ and IZ and mean thickness of the IZ on OCT B-scans with delayed RMDA. The underlying pathophysiology model for ALSTAR2 rests on the tight foveal centration of soft drusen buildup throughout adulthood, as documented by epidemiology[37,38] and confirmed with OCT[39] and histology.[40–42] This configuration in turn is believed to reflect the high metabolic demand of foveal cones and the transfer of xanthophyll pigment across the RPE, with concomitant release of unneeded lipids back to the circulation.[41] The RMDA test spot at 5 degrees lies in an area of rod loss in aging and AMD eyes, on the perimeter of this high-risk area.[42] The 1993 findings from Bird and colleagues of delayed RMDA were measured at 3 degrees from the foveal center.[43] Previous structure-function studies of the retina, in which function is measured by psychophysical responses, typically yield correlations of 0.2 to 0.5.[44–46] We found similar or larger associations between delayed RMDA and the analyzed imaging biomarkers, with the area of discernible IZ demonstrating the strongest association. This association was also found in the cone-dominant central subfield.

Previously, A.Y. Lee et al. using a deep learning model demonstrated that delayed RMDA on foveal OCT B-scans is most impacted by OCT pixels superficial and deep to both the EZ and the RPE-BrM band.[47] This finding led us to investigate the discernability of both the EZ and the IZ areas on OCT in this study. The model utilized by Lee et al. demonstrated a stronger correlation ($r = 0.69$) between variable reflectivity of these hyporeflective bands and delayed RMDA[47] than any of the correlations we calculated between delayed RMDA and discernible EZ or IZ area. However, the strength of the correlation between the IZ area in the entire ETDRS grid and RMDA from this study ($r = 0.591$) was close to that in this previous study. Conversely, correlation with EZ area was notably weaker ($r = 0.334$). The Lee et al. study was limited by evaluating only a single B-scan through the fovea, whereas RIT is measured at 5 degrees eccentricity,[47] which may explain the discrepancy between that study and this one. This is because pathologic changes in AMD, such as changes that precede drusen formation, occur most prominently under the fovea.[38–41] Pathology under the cone-rich fovea can impact rods in the nearby perifovea where RIT was measured.[48] As a result, structural changes in the outer

Investigative Ophthalmology & Visual Science

retina seen at the fovea may be associated with delayed RMDA. However, our analysis showed slightly weaker correlations in the central foveal subfield of the ETDRS grid than the entire ETDRS grid between the retinal structures we analyzed and RMDA.

The association with the IZ thickness differed from the IZ area mainly because of the relatively small area of missing the IZ area in our dataset and the relatively low image quality of spectral domain OCT, resulting in more grading noise for IZ area than thickness. In this initial study, the IZ area was verified as an early AMD biomarker. Further investigation for accurate relationships of the IZ area with different stages of AMD are needed and higher resolution spectral domain OCTs or adaptive optics assisted OCTs are suggested for future image capture. The weaker relationship of the IZ thickness with normal eyes is consistent with our recent findings in a subset of ALSTAR2 participants compared to young normal retinas and may reflect the fact that IZ discernibility is an aging effect for which most change occurs before age 60 years.[49]

In aged and AMD eyes, histopathologic studies have demonstrated preferential loss of rod cells in the central area of eyes with early disease compared with age-matched controls. The greatest loss occurred in the region 0.5 to 3 mm from the fovea.[35] This region aligns with the inner and outer rings of the ETDRS grid, where the structure-function association between the RMDA and the IZ area was strongest with all eyes considered. However, when considering each AREDS category separately, we found the structure-function association was strongest in the outer ring, which contains the RMDA test point (5 degrees eccentricity on the superior vertical meridian), rather than the inner ring or central subfield. This suggests that the observed structure-function association is related to local activity in the outer retina rather than simply a coincident delay in RMDA and decrease in discernible IZ across the entire macula. Additionally, in eyes without AMD, this association was seen in the outer ring only and not in the inner ring or central subfield, suggesting that the effect of local changes may be independent of AMD progression.

Therefore, it is plausible that delayed RMDA results from either the central macular pathology or the local pathology near the RMDA testing location, or a combination of both. Laíns et al. reported that the presence of any abnormalities (EZ disruption, sub-RPE drusen, SDD, hyper-reflective foci, retinal atrophy, subretinal and intraretinal fluid, fibrosis, choroidal neovascularization, and serous pigment epithelial detachment) within the RMDA test spot (located at the same place as ours), as well as any abnormalities in the macula, were significantly associated with longer RIT and therefore delayed RMDA. This association was stronger with abnormalities at the RMDA test spot,[50] which corresponds to our finding that, in normal and early AMD eyes in which abnormalities in the entire macula are relatively rare, the structure-function relationship between the RMDA and the IZ and EZ areas are stronger in the ETDRS ring containing the RMDA testing spot, as those abnormalities likely contribute to a greater proportion of the loss in the EZ and IZ areas than in intermediate eyes.

We speculate that the same mechanisms may be responsible for both the decrease in IZ discernability and delay in RMDA. RPE outer segments and apical processes containing melanosomes contribute reflectivity to the IZ area[51] and these RPE apical processes also contain many proteins relevant to the retinoid processing pathways.[52] The RPE supports the photoreceptors at the IZ by transferring retinoids required for phototransduction and the availability of retinoids is ultimately rate-limiting for RMDA.[27] Therefore, a reduction of IZ anatomic substrates could delay RMDA. Furthermore, the RPE is thought to undergo structural changes with aging, including loss of melanin.[53] These ideas can now be re-investigated with imaging techniques that incorporate new understanding of how melanosomes and melanolipofuscin in human RPE are vertically compartmentalized.[54,55] It should be noted that we age-adjusted the correlations to better isolate the impact of AMD on the IZ area and the RMDA and eliminate the potentially confounding effect of normal aging.

Strengths of this study include a large sample ($n = 476$) of eyes in a cohort designed to cross-sectionally probe the transition from normal aging to AMD, and a comprehensive OCT analysis of the bands of interest throughout the macula utilizing dense volume scanning (121 B-scans in an 8.6 $\times$ 7.2 mm area). Limitations include a relatively homogenous population dominated by participants of European descent and an OCT analysis restricted to ETDRS regions rather than the exact RMDA test location. On the other hand, it is unclear how wide an area surrounding the test spot may contribute to the measured RMDA.

In conclusion, because RMDA is correlated with the status (area and thickness) of outer retinal bands in normal, early, and intermediate AMD eyes and RMDA is a continuous AMD biomarker, the area and thickness values of these bands can be used as AMD biomarkers as verified by RMDA. The IZ area on OCT fulfills the conditions of a valuable imaging biomarker for early AMD by establishing a structure-function association with delayed RMDA. This relationship is biologically plausible, because retinoid availability and transfer at this interface is rate-limiting for RMDA. The structure-function association of EZ area and RMDA was weaker and likely useful only in later stages of AMD. Further studies demonstrating reproducibility of this association with different methodologies and instruments are needed to demonstrate the utility of IZ integrity as an imaging biomarker. Additionally, future studies assessing other aspects of retinoid availability to the photoreceptors and their relationship to the IZ area, as well as the relationship between RMDA and known features of AMD (SDD, drusen, etc.) that effect the outer retinal layers may offer further support for IZ on OCT as an imaging biomarker for early AMD.

Acknowledgments

Supported by the National Eye Institute of the National Institutes of Health under Award Numbers R01EY029595 and R21EY030619, Research to Prevent Blindness, EyeSight Foundation of Alabama, and the Dorsett Davis Discovery Fund.

Data Availability: The data and code generated during the study are accessible from the corresponding author based on reasonable request and subject to the rule/regulatory of the involved institutes.

Disclosure: **S. Fasih-Ahmad**, None; **Z. Wang**, None; **Z. Mishra**, None; **C. Vatanatham**, None; **M.E. Clark**, None; **T.A. Swain**, None; **C.A. Curcio**, Genentech/Hoffman LaRoche (F), Heidelberg Engineering (F), Regeneron (F), and Novartis (F), Apellis (C), Astellas (C), Boehringer Ingelheim (C), Character Biosciences (C), Osanni (C), and Annexon (C) (outside this project); **C. Owsley**, Johnson & Johnson Vision (C) (outside this

project) and AdaptDx (P); **S.R. Sadda**, 4DMT (C), Alexion (C), Allergan Inc. (C), Alnylam Pharmaceuticals (C), Amgen Inc. (C), Apellis Pharmaceuticals, Inc. (C), Astellas (C), Bayer (C), Healthcare Pharmaceuticals (C), Biogen MA, Inc. (C), Boehringer Ingelheim (C), Carl Zeiss Meditec (C), Catalyst Pharmaceuticals Inc. (C), Centervue Inc. (C), Genentech (C), Gyroscope Therapeutics (C), Heidelberg Engineering (C), Hoffman La Roche, Ltd. (C), Iveric Bio (C), Janssen Pharmaceuticals, Inc. (C), Merck & Co., Inc. (C), Nanoscope (C), Notal Vision Inc. (C), Novartis (C), Optos Inc. (C), Oxurion/Thrombogenics (C), Oyster Point Pharma (C), Pfizer Inc. (C), Regeneron Pharmaceuticals Inc. (C), Samsung Bioepis (C), and Vertex Pharmaceuticals Inc. (C), lectures for Carl Zeiss Meditec, Heidelberg Engineering, Nidek Inc., Novartis Pharma, and Topcon Medical Systems Inc., and Carl Zeiss Meditec (F), and Heidelberg Engineering (F) (outside this project); **Z.J. Hu**, Heidelberg Engineering (F) (outside this project)

References

1. Wong WL, Su X, Li X, et al. Global prevalence of age-related macular degeneration and disease burden projection for 2020 and 2040: a systematic review and meta-analysis. *Lancet Glob Health*. 2014;2:e106–e116.
2. Cimarolli VR, Casten RJ, Rovner BW, Heyl V, Sorensen S, Horowitz A. Anxiety and depression in patients with advanced macular degeneration: current perspectives. *Clin Ophthalmol*. 2016;10:55–63.
3. Markowitz M, Daibert-Nido M, Markowitz SN. Rehabilitation of reading skills in patients with age-related macular degeneration. *Can J Ophthalmol*. 2018;53:3–8.
4. Owsley C, McGwin G, Jr. Driving and age-related macular degeneration. *J Vis Impair Blind*. 2008;102:621–635.
5. Fabre M, Mateo L, Lamaa D, et al. Recent advances in age-related macular degeneration therapies. *Molecules*. 2022;27(16):5089.
6. Rein DB, Wittenborn JS, Burke-Conte Z, et al. Prevalence of age-related macular degeneration in the US in 2019. *JAMA Ophthalmol*. 2022;140:1202–1208.
7. Csaky K, Ferris F, 3rd, Chew EY, Nair P, Cheetham JK, Duncan JL. Report from the NEI/FDA Endpoints Workshop on Age-Related Macular Degeneration and Inherited Retinal Diseases. *Invest Ophthalmol Vis Sci*. 2017;58:3456–3463.
8. Schmidt-Erfurth U, Klimscha S, Waldstein SM, Bogunovic H. A view of the current and future role of optical coherence tomography in the management of age-related macular degeneration. *Eye (Lond)*. 2017;31:26–44.
9. Jaffe GJ, Chakravarthy U, Freund KB, et al. Imaging features associated with progression to geographic atrophy in age-related macular degeneration: classification of Atrophy Meeting Report 5. *Ophthalmol Retina*. 2021;5:855–867.
10. Staurenghi G, Sadda S, Chakravarthy U, Spaide RF, International Nomenclature for Optical Coherence Tomography (IN•OCT) Panel. Proposed lexicon for anatomic landmarks in normal posterior segment spectral-domain optical coherence tomography: the IN•OCT consensus. *Ophthalmology*. 2014;121:1572–1578.
11. Spaide RF, Curcio CA. Anatomical correlates to the bands seen in the outer retina by optical coherence tomography: literature review and model. *Retina*. 2011;31:1609–1619.
12. Weese J, Lorenz C. Four challenges in medical image analysis from an industrial perspective. *Med Image Anal*. 2016;33:44–49.
13. Mishra Z, Ganegoda A, Selicha J, Wang Z, Sadda SR, Hu Z. Automated retinal layer segmentation using graph-based algorithm incorporating deep-learning-derived information. *Sci Rep*. 2020;10:9541.
14. FDA-NIH Biomarker Working Group b. Contents of a biomarker description. *BEST (Biomarkers, EndpointS, and other Tools) Resource*. Silver Spring (MD), Bethesda (MD): US Food and Drug Administration (US); 2020.
15. Hoang QV, Linsenmeier RA, Chung CK, Curcio CA. Photoreceptor inner segments in monkey and human retina: mitochondrial density, optics, and regional variation. *Vis Neurosci*. 2002;19:395–407.
16. Litts KM, Zhang Y, Freund KB, Curcio CA. Optical coherence tomography and histology of age-related macular degeneration support mitochondria as reflectivity sources. *Retina*. 2018;38:445–461.
17. Berkowitz BA, Podolsky RH, Childers KL, et al. Functional changes within the rod inner segment ellipsoid in wild-type mice: an optical coherence tomography and electron microscopy study. *Invest Ophthalmol Vis Sci*. 2022;63:8.
18. Litts KM, Messinger JD, Freund KB, Zhang Y, Curcio CA. Inner segment remodeling and mitochondrial translocation in cone photoreceptors in age-related macular degeneration with outer retinal tubulation. *Invest Ophthalmol Vis Sci*. 2015;56:2243–2253.
19. Riazi-Esfahani M, Kuppermann BD, Kenney MC. The role of mitochondria in AMD: current knowledge and future applications. *J Ophthalmic Vis Res*. 2017;12:424–428.
20. Terluk MR, Kapphahn RJ, Soukup LM, et al. Investigating mitochondria as a target for treating age-related macular degeneration. *J Neurosci*. 2015;35:7304–7311.
21. Xie W, Zhao M, Tsai SH, et al. Correlation of spectral domain optical coherence tomography with histology and electron microscopy in the porcine retina. *Exp Eye Res*. 2018;177:181–190.
22. Nawrot M, West K, Huang J, et al. Cellular retinaldehyde-binding protein interacts with ERM-binding phosphoprotein 50 in retinal pigment epithelium. *Invest Ophthalmol Vis Sci*. 2004;45:393–401.
23. Owsley C, McGwin G, Jr., Clark ME, et al. Delayed rod-mediated dark adaptation is a functional biomarker for incident early age-related macular degeneration. *Ophthalmology*. 2016;123:344–351.
24. Linton JD, Holzhausen LC, Babai N, et al. Flow of energy in the outer retina in darkness and in light. *Proc Natl Acad Sci USA*. 2010;107:8599–8604.
25. Yang GQ, Chen T, Tao Y, Zhang ZM. Recent advances in the dark adaptation investigations. *Int J Ophthalmol*. 2015;8:1245–1252.
26. Kaynezhad P, Tachtsidis I, Sivaprasad S, Jeffery G. Watching the human retina breath in real time and the slowing of mitochondrial respiration with age. *Sci Rep*. 2023;13:6445.
27. Lamb TD, Pugh EN, Jr. Dark adaptation and the retinoid cycle of vision. *Prog Retin Eye Res*. 2004;23:307–380.
28. Lamb TD, Pugh EN, Jr. Phototransduction, dark adaptation, and rhodopsin regeneration the proctor lecture. *Invest Ophthalmol Vis Sci*. 2006;47:5137–5152.
29. Ehlers JP, Zahid R, Kaiser PK, et al. Longitudinal assessment of ellipsoid zone integrity, subretinal hyperreflective material, and subretinal pigment epithelium disease in neovascular age-related macular degeneration. *Ophthalmol Retina*. 2021;5:1204–1213.
30. Sadda SR, Joeres S, Wu Z, et al. Error correction and quantitative subanalysis of optical coherence tomography data using computer-assisted grading. *Invest Ophthalmol Vis Sci*. 2007;48:839–848.
31. Joeres S, Tsong JW, Updike PG, et al. Reproducibility of quantitative optical coherence tomography subanalysis in neovascular age-related macular degeneration. *Invest Ophthalmol Vis Sci*. 2007;48:4300–4307.
32. Nittala MG, Ruiz-Garcia H, Sadda SR. Accuracy and reproducibility of automated drusen segmentation in eyes with non-neovascular age-related macular degeneration. *Invest Ophthalmol Vis Sci*. 2012;53:8319–8324.

Investigative Ophthalmology & Visual Science

33. Early Treatment Diabetic Retinopathy Study Research Group. Grading diabetic retinopathy from stereoscopic color fundus photographs–an extension of the modified Airlie House classification. ETDRS report number 10. *Ophthalmology*. 1991;98:786–806.
34. Curcio CA, Millican CL, Allen KA, Kalina RE. Aging of the human photoreceptor mosaic: evidence for selective vulnerability of rods in central retina. *Invest Ophthalmol Vis Sci*. 1993;34:3278–3296.
35. Curcio CA, Medeiros NE, Millican CL. Photoreceptor loss in age-related macular degeneration. *Invest Ophthalmol Vis Sci*. 1996;37:1236–1249.
36. Davis MD, Gangnon RE, Lee LY, et al. The Age-Related Eye Disease Study severity scale for age-related macular degeneration: AREDS Report No. 17. *Arch Ophthalmol*. 2005;123:1484–1498.
37. Wang Q, Chappell RJ, Klein R, et al. Pattern of age-related maculopathy in the macular area. The Beaver Dam Eye Study. *Invest Ophthalmol Vis Sci*. 1996;37:2234–2242.
38. Wang JJ, Rochtchina E, Lee AJ, et al. Ten-year incidence and progression of age-related maculopathy: the Blue Mountains Eye Study. *Ophthalmology*. 2007;114:92–98.
39. Pollreisz A, Reiter GS, Bogunovic H, et al. Topographic distribution and progression of soft drusen volume in age-related macular degeneration implicate neurobiology of fovea. *Invest Ophthalmol Vis Sci*. 2021;62:26.
40. Chen L, Messinger JD, Kar D, Duncan JL, Curcio CA. Biometrics, impact, and significance of basal linear deposit and subretinal drusenoid deposit in age-related macular degeneration. *Invest Ophthalmol Vis Sci*. 2021;62:33.
41. Sura AA, Chen L, Messinger JD, et al. Measuring the contributions of basal laminar deposit and Bruch's membrane in age-related macular degeneration. *Invest Ophthalmol Vis Sci*. 2020;61:19.
42. Rudolf M, Malek G, Messinger JD, Clark ME, Wang L, Curcio CA. Sub-retinal drusenoid deposits in human retina: organization and composition. *Exp Eye Res*. 2008;87:402–408.
43. Steinmetz RL, Haimovici R, Jubb C, Fitzke FW, Bird AC. Symptomatic abnormalities of dark adaptation in patients with age-related Bruch's membrane change. *Br J Ophthalmol*. 1993;77:549–554.
44. Flamendorf J, Agron E, Wong WT, et al. Impairments in dark adaptation are associated with age-related macular degeneration severity and reticular pseudodrusen. *Ophthalmology*. 2015;122:2053–2062.
45. Sevilla MB, McGwin G, Jr., Lad EM, et al. Relating retinal morphology and function in aging and early to intermediate age-related macular degeneration subjects. *Am J Ophthalmol*. 2016;165:65–77.
46. Acton JH, Smith RT, Hood DC, Greenstein VC. Relationship between retinal layer thickness and the visual field in early age-related macular degeneration. *Invest Ophthalmol Vis Sci*. 2012;53:7618–7624.
47. Lee AY, Lee CS, Blazes MS, et al. Exploring a structural basis for delayed rod-mediated dark adaptation in age-related macular degeneration via deep learning. *Transl Vis Sci Technol*. 2020;9:62.
48. Curcio CA. Antecedents of soft drusen, the specific deposits of age-related macular degeneration, in the biology of human macula. *Invest Ophthalmol Vis Sci*. 2018;59:AMD182–AMD194.
49. Berlin A, Matney E, Jones SG, et al. Discernibility of the interdigitation zone (IZ), a potential optical coherence tomography (OCT) biomarker for visual dysfunction in aging. *Curr Eye Res*. 2023;48:1050–1056.
50. Lains I, Miller JB, Park DH, et al. Structural changes associated with delayed dark adaptation in age-related macular degeneration. *Ophthalmology*. 2017;124:1340–1352.
51. Zhang QX, Lu RW, Messinger JD, Curcio CA, Guarcello V, Yao XC. In vivo optical coherence tomography of light-driven melanosome translocation in retinal pigment epithelium. *Sci Rep*. 2013;3:2644.
52. Bonilha VL, Bhattacharya SK, West KA, et al. Support for a proposed retinoid-processing protein complex in apical retinal pigment epithelium. *Exp Eye Res*. 2004;79:419–422.
53. Boulton M, Dayhaw-Barker P. The role of the retinal pigment epithelium: topographical variation and ageing changes. *Eye (Lond)*. 2001;15:384–389.
54. Pollreisz A, Neschi M, Sloan KR, et al. Atlas of human retinal pigment epithelium organelles significant for clinical imaging. *Invest Ophthalmol Vis Sci*. 2020;61:13.
55. Lindell M, Kar D, Sedova A, et al. Volumetric reconstruction of a human retinal pigment epithelial cell reveals specialized membranes and polarized distribution of organelles. *Invest Ophthalmol Vis Sci*. 2023;64(15):35.

Investigative Ophthalmology & Visual Science